Power-Management Strategies for a Grid-Connected PV-FC Hybrid System

Loc Nguyen Khanh, *Student Member, IEEE*, Jae-Jin Seo, Yun-Seong Kim, and Dong-Jun Won, *Member, IEEE*

***Abstract*—This paper presents a method to operate a grid connected hybrid system. The hybrid system composed of a Photovoltaic (PV) array and a Proton exchange membrane fuel cell (PEMFC) is considered. The PV array normally uses a maximum power point tracking (MPPT) technique to continuously deliver the highest power to the load when variations in irradiation and temperature occur, which make it become an uncontrollable source. In coordination with PEMFC, the hybrid system output power becomes controllable. Two operation modes, the unit-power control (UPC) mode and the feeder-flow control (FFC) mode, can be applied to the hybrid system. The coordination of two control modes, the coordination of the PV array and the PEMFC in the hybrid system, and the determination of reference parameters are presented. The proposed operating strategy with a flexible operation mode change always operates the PV array at maximum output power and the PEMFC in its high efficiency performance band, thus improving the performance of system operation, enhancing system stability, and decreasing the number of operating mode changes.**

***Index Terms*—Distributed generation, fuel cell, hybrid system, microgrid, photovoltaic, power management.**

NOMENCLATURE

A	A dimensionless factor.
D	Duty cycle.
f	Switching frequency.
F	Faraday constant (96487 coulombs per mol).
G_a	Irradiation (W/m^2).
G_{as}	Standard irradiation (1000 W/m^2).
$I_{\rm sc}$	Short-circuit current.
$I_{\rm ph}$	Photo current.
$I_{\rm sat}$	Reverse saturation current.
$I_{\rm limit}$	Limitation current (in amperes).
K	Boltzmann constant.
$P_{\rm PV}$	Photovoltaic output power.
P_{MPP}	PV maximum output power.
$P_{\rm FC}$	PEMFC output power.
$P_{\rm FC}^{\rm low}$	PEMFC lower limit of high efficiency band.
$P_{\rm FC}^{\rm up}$	PEMFC upper limit of high efficiency band.
$P_{\rm FC}^{\rm max}$	PEMFC maximum output power.
$P_{\rm Feeder}$	Feeder power flow.
$P_{\rm Feeder}^{\rm ref}$	Feeder reference power.
$P_{\rm Feeder}^{\rm max}$	Feeder maximum power.
$P_{\rm MS}^{\rm ref}$	Hybrid source reference power.
$P_{\rm Load}$	Load demand.
q	Electronic charge.
R	Gas constant, 8.3143 J/(mol.K).
R_s	Series resistance.
T	Temperature (in Kelvin).
T_s	Standard temperature (298 K).
V_t	Thermal voltage.
$V_{\rm op}$	Open-circuit voltage.
Z	Number of participating electrons.
$\Delta I_{\rm sc}$	Temperature coefficient.
$\Delta V/V_0$	Voltage ripples.

Manuscript received July 13, 2009; revised December 10, 2009, March 10, 2010. First published May 18, 2010; current version published June 23, 2010. This work was supported by an INHA University Research Grant. Paper no. TPWRD-00523-2009.

The authors are with the Department of Electrical Engineering, Inha University, Incheon 402-751, Korea (e-mail: djwon@inha.ac.kr).

Color versions of one or more of the figures in this paper are available online at http://ieeexplore.ieee.org.

Digital Object Identifier 10.1109/TPWRD.2010.2047735

I. INTRODUCTION

RENEWABLE energy is currently widely used. One of these resources is solar energy. The photovoltaic (PV) array normally uses a maximum power point tracking (MPPT) technique to continuously deliver the highest power to the load when there are variations in irradiation and temperature. The disadvantage of PV energy is that the PV output power depends on weather conditions and cell temperature, making it an uncontrollable source. Furthermore, it is not available during the night. In order to overcome these inherent drawbacks, alternative sources, such as PEMFC, should be installed in the hybrid system. By changing the FC output power, the hybrid source output becomes controllable. However, PEMFC, in its turn, works only at a high efficiency within a specific power range $(P_{\rm FC}^{\rm low} \div P_{\rm FC}^{\rm up})$ [1], [2].

The hybrid system can either be connected to the main grid or work autonomously with respect to the grid-connected mode or islanded mode, respectively. In the grid-connected mode,

the hybrid source is connected to the main grid at the point of common coupling (PCC) to deliver power to the load. When load demand changes, the power supplied by the main grid and hybrid system must be properly changed. The power delivered from the main grid and PV array as well as PEMFC must be coordinated to meet load demand. The hybrid source has two control modes: 1) unit-power control (UPC) mode and feeder-flow control (FFC) mode. In the UPC mode, variations of load demand are compensated by the main grid because the hybrid source output is regulated to reference power. Therefore, the reference value of the hybrid source output $P_{\rm MS}^{\rm ref}$ must be determined. In the FFC mode, the feeder flow is regulated to a constant, the extra load demand is picked up by the hybrid source, and, hence, the feeder reference power $P_{\rm feeder}^{\rm ref}$ must be known.

The proposed operating strategy is to coordinate the two control modes and determine the reference values of the UPC mode and FFC mode so that all constraints are satisfied. This operating strategy will minimize the number of operating mode changes, improve performance of the system operation, and enhance system stability.

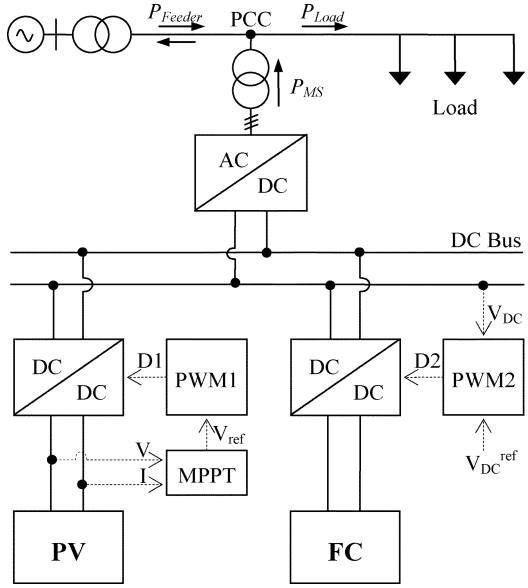

Fig. 1. Grid-connected PV-FC hybrid system.

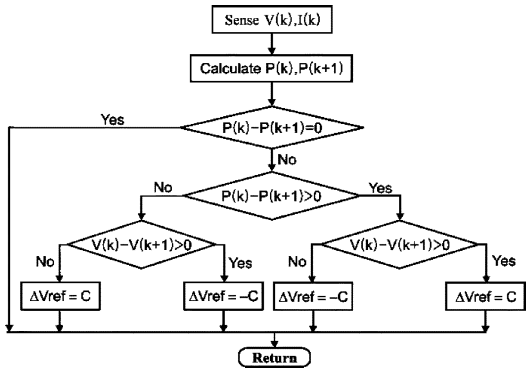

Fig. 2. P&O MPPT algorithm.

II. System Description

A. Structure of Grid-Connected Hybrid Power System

The system consists of a PV-FC hybrid source with the main grid connecting to loads at the PCC as shown in Fig. 1. The photovoltaic [3], [4] and the PEMFC [5], [6] are modeled as nonlinear voltage sources. These sources are connected to dc–dc converters which are coupled at the dc side of a dc/ac inverter. The dc/dc connected to the PV array works as an MPPT controller. Many MPPT algorithms have been proposed in the literature, such as incremental conductance (INC), constant voltage (CV), and perturbation and observation (P&O). The P&O method has been widely used because of its simple feedback structure and fewer measured parameters [7]. The P&O algorithm with power feedback control [8]–[10] is shown in Fig. 2. As PV voltage and current are determined, the power is calculated. At the maximum power point, the derivative (dP/dV) is equal to zero. The maximum power point can be achieved by changing the reference voltage by the amount of $\Delta V_{\rm ref}$.

B. PV Array Model

The mathematical model [3], [4] can be expressed as

$$I = I_{\rm ph} - I_{\rm sat}\left\{\exp\left[\frac{q}{AKT}(V + IR_s)\right] - 1\right\}. \quad (1)$$

Equation (1) shows that the output characteristic of a solar cell is nonlinear and vitally affected by solar radiation, temperature, and load condition.

Photocurrent $I_{\rm ph}$ is directly proportional to solar radiation $\rm G_a$

$$I_{\rm ph}(G_a) = I_{\rm sc}\frac{G_a}{G_{\rm as}}. \quad (2)$$

The short-circuit current of solar cell $I_{\rm sc}$ depends linearly on cell temperature

$$I_{\rm sc}(T) = I_{scs}[1 + \Delta I_{\rm sc}(T - T_s)]. \quad (3)$$

Thus, $I_{\rm ph}$ depends on solar irradiance and cell temperature

$$I_{\rm ph}(G_a, T) = I_{scs}\frac{G_a}{G_{\rm as}}[1 + \Delta I_{\rm sc}(T - T_s)]. \quad (4)$$

$I_{\rm sat}$ also depends on solar irradiation and cell temperature and can be mathematically expressed as follows:

$$I_{\rm sat}(G_a, T) = \frac{I_{\rm ph}(G_a, T)}{e^{\left(\frac{V_{\rm oc}(T)}{V_t(T)}\right)} - 1}. \quad (5)$$

C. PEMFC Model

The PEMFC steady-state feature of a PEMFC source is assessed by means of a polarization curve, which shows the nonlinear relationship between the voltage and current density. The PEMFC output voltage is as follows [5]:

$$V_{\rm out} = E_{\rm Nerst} - V_{\rm act} - V_{\rm ohm} - V_{\rm conc} \quad (6)$$

where $E_{\rm Nerst}$ is the "thermodynamic potential" of Nerst, which represents the reversible (or open-circuit) voltage of the fuel

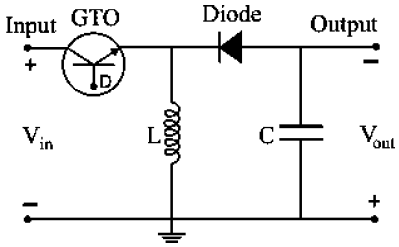

Fig. 3. Buck-boost topology.

cell. Activation voltage drop $V_{\rm act}$ is given in the Tafel equation as

$$V_{\rm act} = T[a + bln(I)] \tag{7}$$

where a, b are the constant terms in the Tafel equation (in volts per Kelvin)

The overall ohmic voltage drop $V_{\rm ohm}$ can be expressed as

$$V_{\rm ohm} = IR_{\rm ohm}. \tag{8}$$

The ohmic resistance $R_{\rm ohm}$ of PEMFC consists of the resistance of the polymer membrane and electrodes, and the resistances of the electrodes.

The concentration voltage drop $V_{\rm conc}$ is expressed as

$$V_{\rm conc} = -\frac{RT}{zF} ln\left(1 - \frac{I}{I_{\rm limit}}\right). \tag{9}$$

D. MPPT Control

Many MPPT algorithms have been proposed in the literature, such as incremental conductance (INC), constant voltage (CV), and perturbation and observation (P&O). The two algorithms often used to achieve maximum power point tracking are the P&O and INC methods. The INC method offers good performance under rapidly changing atmospheric conditions. However, four sensors are required to perform the computations. If the sensors require more conversion time, then the MPPT process will take longer to track the maximum power point. During tracking time, the PV output is less than its maximum power. This means that the longer the conversion time is, the larger amount of power loss [7] will be. On the contrary, if the execution speed of the P&O method increases, then the system loss will decrease. Moreover, this method only requires two sensors, which results in a reduction of hardware requirements and cost. Therefore, the P&O method is used to control the MPPT process.

In order to achieve maximum power, two different applied control methods that are often chosen are voltage-feedback control and power-feedback control [8], [9]. Voltage-feedback control uses the solar-array terminal voltage to control and keep the array operating near its maximum power point by regulating the array's voltage and matching the voltage of the array to a desired voltage. The drawback of the voltage-feedback control is its neglect of the effect of irradiation and cell temperature. Therefore, the power-feedback control is used to achieve maximum power. The P&O MPPT algorithm with a power-feedback control [9], [10] is shown in Fig. 2. As PV voltage and current are determined, the power is calculated. At the maximum power point, the derivative (dP/dV) is equal to zero. The maximum power point can be achieved by changing the reference voltage by the amount of $\Delta V_{\rm ref}$.

In order to implement the MPPT algorithm, a buck-boost dc/dc converter is used as depicted in Fig. 3.

The parameters L and C in the buck-boost converter must satisfy the following conditions [11]:

$$L > \frac{(1-D)^2 R}{2f} \quad ; \quad C > \frac{D}{Rf(\Delta V/V_{\rm out})}. \tag{10}$$

The buck-boost converter consists of one switching device (GTO) that enables it to turn on and off depending on the applied gate signal D. The gate signal for the GTO can be obtained by comparing the sawtooth waveform with the control voltage [7]. The change of the reference voltage $\Delta V_{\rm ref}$ obtained by MPPT algorithm becomes the input of the pulsewidth modulation (PWM). The PWM generates a gate signal to control the buck-boost converter and, thus, maximum power is tracked and delivered to the ac side via a dc/ac inverter.

III. Control of The Hybrid System

The control modes in the microgrid include unit power control, feeder flow control, and mixed control mode. The two control modes were first proposed by Lasserter [12].

In the UPC mode, the DGs (the hybrid source in this system) regulate the voltage magnitude at the connection point and the power that source is injecting. In this mode if a load increases anywhere in the microgrid, the extra power comes from the grid, since the hybrid source regulates to a constant power. In the FFC mode, the DGs regulate the voltage magnitude at the connection point and the power that is flowing in the feeder at connection point $P_{\rm feeder}$. With this control mode, extra load demands are picked up by the DGs, which maintain a constant load from the utility viewpoint. In the mixed control mode, the same DG could control either its output power or the feeder flow power. In other words, the mixed control mode is a coordination of the UPC mode and the FFC mode.

Both of these concepts were considered in [13]–[16]. In this paper, a coordination of the UPC mode and the FFC mode was investigated to determine when each of the two control modes was applied and to determine a reference value for each mode. Moreover, in the hybrid system, the PV and PEMFC sources have their constraints. Therefore, the reference power must be set at an appropriate value so that the constraints of these sources are satisfied. The proposed operation strategy presented in the next section is also based on the minimization of mode change. This proposed operating strategy will be able to improve performance of the system's operation and enhance system stability.

IV. Operating Strategy of The Hybrid System

As mentioned before, the purpose of the operating algorithm is to determine the control mode of the hybrid source and the reference value for each control mode so that the PV is able to work at maximum output power and the constraints are fulfilled. Once the constraints ($P_{\rm FC}^{\rm low}$, $P_{\rm FC}^{\rm up}$, and $P_F^{\rm max}$) are known, the control mode of the hybrid source (UPC mode and FFC mode) depends

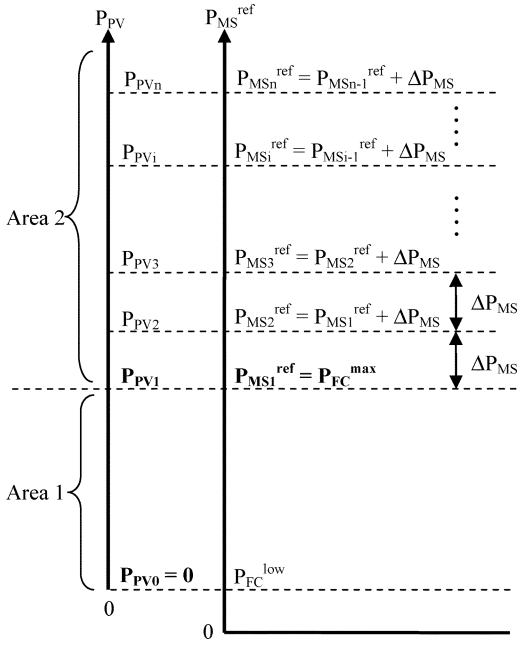

Fig. 4. Operation strategy of hybrid source in the UPC mode.

on load variations and the PV output. The control mode is decided by the algorithm shown in Fig. 7, Subsection B. In the UPC mode, the reference output power of the hybrid source $P_{\rm MS}^{\rm ref}$ depends on the PV output and the constraints of the FC output. The algorithm determining $P_{\rm MS}^{\rm ref}$ is presented in Subsection A and is depicted in Fig. 4.

A. Operating Strategy for the Hybrid System in the UPC Mode

In this subsection, the presented algorithm determines the hybrid source works in the UPC mode. This algorithm allows the PV to work at its maximum power point, and the FC to work within its high efficiency band.

In the UPC mode, the hybrid source regulates the output to the reference value. Then

$$P_{\rm PV} + P_{\rm FC} = P_{\rm MS}^{\rm ref}. \tag{11}$$

Equation (11) shows that the variations of the PV output will be compensated for by the FC power and, thus, the total power will be regulated to the reference value. However, the FC output must satisfy its constraints and, hence, $P_{\rm MS}^{\rm ref}$ must set at an appropriate value. Fig. 4 shows the operation strategy of the hybrid source in UPC mode to determine $P_{\rm MS}^{\rm ref}$. The algorithm includes two areas: Area 1 and Area 2.

In Area 1, $P_{\rm PV}$ is less than $P_{\rm PV1}$, and then the reference power $P_{\rm MS1}^{\rm ref}$ is set at $P_{\rm FC}^{\rm up}$ where

$$P_{\rm PV1} = P_{\rm FC}^{\rm up} - P_{\rm FC}^{\rm low} \tag{12}$$

$$P_{\rm MS1}^{\rm ref} = P_{\rm FC}^{\rm up}. \tag{13}$$

If PV output is zero, then (11) deduces $P_{\rm FC}$ to be equal to $P_{\rm FC}^{\rm up}$. If the PV output increases to $P_{\rm PV1}$, then from (11) and (12), we obtain $P_{\rm FC}$ equal to $P_{\rm FC}^{\rm low}$. In other words, when the PV output varies from zero to $P_{\rm PV1}$, the FC output will change from $P_{\rm FC}^{\rm up}$ to $P_{\rm FC}^{\rm low}$. As a result, the constraints for the FC output always reach Area 1. It is noted that the reference power of the hybrid source during the UPC mode is fixed at a constant $P_{\rm FC}^{\rm up}$.

Area 2 is for the case in which PV output power is greater than $P_{\rm PV1}$. As examined earlier, when the PV output increases to $P_{\rm PV1}$, the FC output will decrease to its lower limit $P_{\rm FC}^{\rm low}$. If PV output keeps increasing, the FC output will decrease below its limit $P_{\rm FC}^{\rm low}$. In this case, to operate the PV at its maximum power point and the FC within its limit, the reference power must be increased. As depicted in Fig. 4, if PV output is larger than $P_{\rm PV1}$, the reference power will be increased by the amount of $\Delta P_{\rm MS}$, and we obtain

$$P_{\rm MS2}^{\rm ref} = P_{\rm MS1}^{\rm ref} + \Delta P_{\rm MS}. \tag{14}$$

Similarly, if $P_{\rm PV}$ is greater than $P_{\rm PV2}$, the FC output becomes less than its lower limit and the reference power will be thus increased by the amount of $\Delta P_{\rm MS}$. In other words, the reference power remains unchanged and equal to $P_{\rm MS2}^{\rm ref}$ if $P_{\rm PV}$ is less than $P_{\rm PV2}$ and greater than $P_{\rm PV1}$ where

$$P_{\rm PV2} = P_{\rm PV1} + \Delta P_{\rm MS} \tag{15}$$

it is noted that $\Delta P_{\rm MS}$ is limited so that with the new reference power, the FC output must be less than its upper limit $P_{\rm FC}^{\rm up}$. Then, we have

$$\Delta P_{\rm MS} \le P_{\rm FC}^{\rm up} - P_{\rm FC}^{\rm low}. \tag{16}$$

In general, if the PV output is between $P_{\rm PVi}$ and $P_{{\rm PV}i-1}$ $(i = 2, 3, 4\ldots)$, then we have

$$P_{{\rm MS}i}^{\rm ref} = P_{{\rm MS}i-1}^{\rm ref} + \Delta P_{\rm MS} \tag{17}$$

$$P_{{\rm PV}i} = P_{{\rm PV}i-1} + \Delta P_{\rm MS}. \tag{18}$$

Equations (17) and (18) show the method of finding the reference power when the PV output is in Area 2. The relationship between $P_{{\rm MS}i}^{\rm ref}$ and $P_{{\rm PV}i}$ is obtained by using (12), (13), and (18) in (17), and then

$$P_{{\rm MS}i}^{\rm ref} = P_{{\rm PV}i} + P_{\rm FC}^{\rm min}, \quad i = 2, 3, 4\ldots \tag{19}$$

The determination of $P_{\rm MS}^{\rm ref}$ in Area 1 and Area 2 can be generalized by starting the index i from 1. Therefore, if the PV output is

$$P_{{\rm PV}i-1} \le P_{\rm PV} \le P_{{\rm PV}i}, \quad i = 1, 2, 3\ldots$$

then we have

$$P_{{\rm MS}i}^{\rm ref} = P_{{\rm PV}i} + P_{\rm FC}^{\rm min}, \quad i = 1, 2, 3\ldots \tag{20}$$

$$P_{{\rm PV}i} = P_{{\rm PV}i-1} + \Delta P_{\rm MS}, \quad i = 2, 3, 4\ldots \tag{21}$$

it is noted that when $i = 1$, $P_{\rm PV1}$ is given in (12), and

$$P_{{\rm PV}i-1} = P_{\rm PV0} = 0. \tag{22}$$

In brief, the reference power of the hybrid source is determined according to the PV output power. If the PV output is in Area 1, the reference power will always be constant and set at $P_{\rm FC}^{\rm up}$. Otherwise, the reference value will be changed by the amount of $\Delta P_{\rm MS}$, according to the change of PV power. The

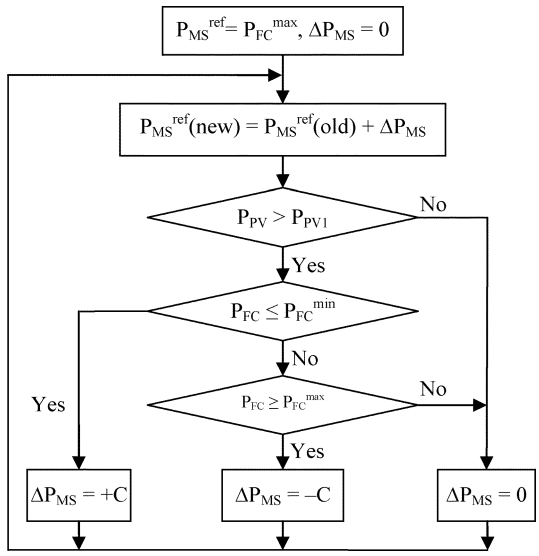

Fig. 5. Control algorithm diagram in the UPC mode ($P_{\mathrm{MS}}^{\mathrm{ref}}$ automatically changing).

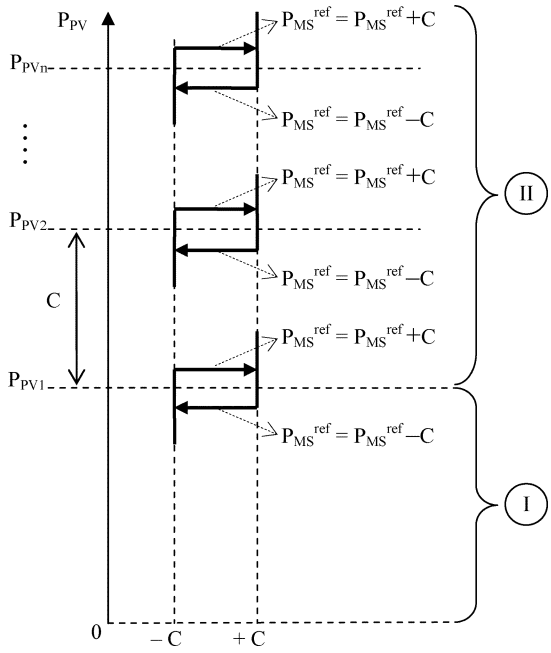

Fig. 6. Hysteresis control scheme for $P_{\mathrm{MS}}^{\mathrm{ref}}$ control.

reference power of the hybrid source $P_{\mathrm{MS}}^{\mathrm{ref}}$ in Area 1 and Area 2 is determined by (20) and (21). $P_{\mathrm{PV0}}, P_{\mathrm{PV1}}$, and ΔP_{MS} are shown in (22), (12), and (16), respectively.

Fig. 5. shows the control algorithm diagram for determining the reference power automatically. The constant C must satisfy (16). If C increases the number of change of $P_{\mathrm{MS}}^{\mathrm{ref}}$ will decrease and thus the performance of system operation will be improved. However, C should be small enough so that the frequency does not change over its limits ($\pm 5\%$).

In order to improve the performance of the algorithm, a hysteresis is included in the simulation model. The hysteresis is used to prevent oscillation of the setting value of the hybrid system reference power $P_{\mathrm{MS}}^{\mathrm{ref}}$. At the boundary of change in $P_{\mathrm{MS}}^{\mathrm{ref}}$, the reference value will be changed continuously due to the oscillations in PV maximum power tracking. To avoid the oscillations around the boundary, a hysteresis is included and its control scheme to control $P_{\mathrm{MS}}^{\mathrm{ref}}$ is depicted in Fig. 6.

B. Overall Operating Strategy for the Grid-Connected Hybrid System

It is well known that in the microgrid, each DG as well as the hybrid source has two control modes: 1) the UPC mode and 2) the FFC mode. In the aforementioned subsection, a method to determine $P_{\mathrm{MS}}^{\mathrm{ref}}$ in the UPC mode is proposed. In this subsection, an operating strategy is presented to coordinate the two control modes. The purpose of the algorithm is to decide when each control mode is applied and to determine the reference value of the feeder flow when the FFC mode is used. This operating strategy must enable the PV to work at its maximum power point, FC output, and feeder flow to satisfy their constraints.

If the hybrid source works in the UPC mode, the hybrid output is regulated to a reference value and the variations in load are matched by feeder power. With the reference power $P_{\mathrm{MS}}^{\mathrm{ref}}$ proposed in Subsection A, the constraints of FC and PV are always satisfied. Therefore, only the constraint of feeder flow is considered. On the other hand, when the hybrid works in the FFC mode, the feeder flow is controlled to a reference value $P_{\mathrm{feeder}}^{\mathrm{ref}}$

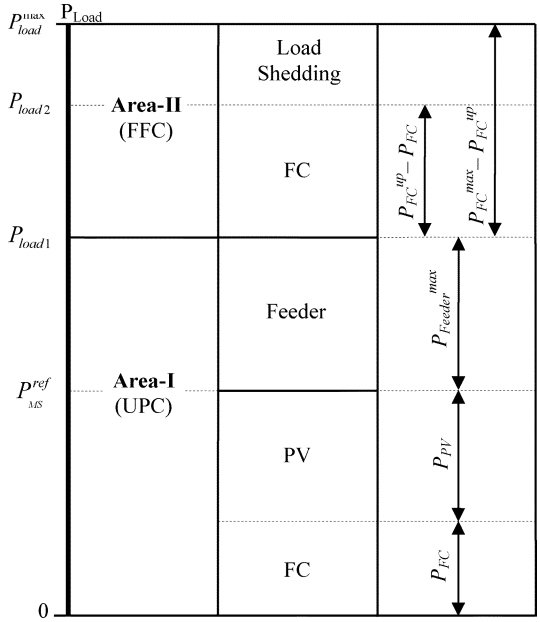

Fig. 7. Overall operating strategy for the grid-connected hybrid system.

and, thus, the hybrid source will compensate for the load variations. In this case, all constraints must be considered in the operating algorithm. Based on those analyses, the operating strategy of the system is proposed as demonstrated in Fig. 7.

The operation algorithm in Fig. 7 involves two areas (Area I and Area II) and the control mode depends on the load power. If load is in Area I, the UPC mode is selected. Otherwise, the FFC mode is applied with respect to Area II.

In the UPC area, the hybrid source output is $P_{\mathrm{MS}}^{\mathrm{ref}}$. If the load is lower than $P_{\mathrm{MS}}^{\mathrm{ref}}$, the redundant power will be transmitted to the main grid. Otherwise, the main grid will send power to the load side to match load demand. When load increases, the feeder

flow will increase correspondingly. If feeder flow increases to its maximum $P_{\text{feeder}}^{\max}$, then the feeder flow cannot meet load demand if the load keeps increasing. In order to compensate for the load demand, the control mode must be changed to FFC with respect to Area II. Thus, the boundary between Area I and Area II P_{load1} is

$$P_{\text{Load1}} = P_{\text{Feeder}}^{\max} + P_{\text{MS}}^{\text{ref}}. \tag{23}$$

When the mode changes to FFC, the feeder flow reference must be determined. In order for the system operation to be seamless, the feeder flow should be unchanged during control mode transition. Accordingly, when the feeder flow reference is set at $P_{\text{feeder}}^{\max}$, then we have

$$P_{\text{Feeder}}^{\text{ref}} = P_{\text{Feeder}}^{\max}. \tag{24}$$

In the FFC area, the variation in load is matched by the hybrid source. In other words, the changes in load and PV output are compensated for by PEMFC power. If the FC output increases to its upper limit and the load is higher than the total generating power, then load shedding will occur. The limit that load shedding will be reached is

$$P_{\text{Load2}} = P_{\text{FC}}^{\text{up}} + P_{\text{Feeder}}^{\max} + P_{\text{PV}}. \tag{25}$$

Equation (25) shows that P_{load2} is minimal when PV output is at 0 kW. Then

$$P_{\text{Load2}}^{\min} = P_{\text{FC}}^{\text{up}} + P_{\text{Feeder}}^{\max}. \tag{26}$$

Equation (26) means that if load demand is less than $P_{\text{load2}}^{\min}$, load shedding will never occur.

From the beginning, FC has always worked in the high efficiency band and FC output has been less than $P_{\text{FC}}^{\text{up}}$. If the load is less than $P_{\text{load2}}^{\min}$, load shedding is ensured not to occur. However, in severe conditions, FC should mobilize its availability, $P_{\text{FC}}^{\max}$, to supply the load. Thus, the load can be higher and the largest load is

$$P_{\text{Load}}^{\max} = P_{\text{FC}}^{\max} + P_{\text{Feeder}}^{\max}. \tag{27}$$

If FC power and load demand satisfy (27), load shedding will never occur. Accordingly, based on load forecast, the installed power of FC can be determined by following (27) to avoid load shedding. Corresponding to the FC installed power, the width of Area II is calculated as follows:

$$P_{\text{Area-II}} = P_{\text{FC}}^{\max} - P_{\text{FC}}^{\text{up}}. \tag{28}$$

In order for the system to work more stably, the number of mode changes should be decreased. As seen in Fig. 7, the limit changing the mode from UPC to FFC is P_{Load1}, which is calculated in (23). Equation (23) shows that P_{Load1} depends on $P_{\text{Feeder}}^{\max}$ and $P_{\text{MS}}^{\text{ref}}$. $P_{\text{Feeder}}^{\max}$ is a constant, thus P_{Load1} depends on $P_{\text{MS}}^{\text{ref}}$. Fig. 4 shows that in Area 2 $P_{\text{MS}}^{\text{ref}}$ depends on ΔP_{MS}. Therefore, to decrease the number of mode changes, $P_{\text{MS}}^{\text{ref}}$ changes must be reduced. Thus, ΔP_{MS} must be increased. However, ΔP_{MS} must satisfy condition (16) and, thus, the minimized number of mode change is reached when ΔP_{MS} is maximized

$$\Delta P_{\text{MS}}^{\max} = P_{\text{FC}}^{\text{up}} - P_{\text{FC}}^{\text{low}}. \tag{29}$$

In summary, in a light-load condition, the hybrid source works in UPC mode, the hybrid source regulates output power to the reference value $P_{\text{MS}}^{\text{ref}}$, and the main grid compensates for load variations. $P_{\text{MS}}^{\text{ref}}$ is determined by the algorithm shown in Fig. 4 and, thus, the PV always works at its maximum power point and the PEMFC always works within the high efficiency band ($P_{\text{FC}}^{\text{low}} \div P_{\text{FC}}^{\text{up}}$). In heavy load conditions, the control mode changes to FFC, and the variation of load will be matched by the hybrid source. In this mode, PV still works with the MPPT control, and PEMFC operates within its efficiency band until load increases to a very high point. Hence, FC only works outside the high efficiency band ($P_{\text{FC}}^{\text{up}} \div P_{\text{FC}}^{\max}$) in severe conditions. With an installed power of FC and load demand satisfying (27), load shedding will not occur. Besides, to reduce the number of mode changes, ΔP_{MS} must be increased and, hence, the number of mode changes is minimized when ΔP_{MS} is maximized, as shown in (29). In addition, in order for system operation to be seamless, the reference value of feeder flow must be set at $P_{\text{Feeder}}^{\max}$.

TABLE I
SYSTEM PARAMETERS

Parameter	Value	Unit
P_{FC}^{low}	0.01	MW
P_{FC}^{up}	0.07	MW
P_{Feeder}^{max}	0.01	MW
ΔP_{MS}	0.03	MW

V. SIMULATION RESULT AND DISCUSSION

A. Simulation Results in the Case Without Hysteresis

A simulation was carried out by using the system model shown in Fig. 2 to verify the operating strategies. The system parameters are shown in Table I.

In order to verify the operating strategy, the load demand and PV output were time varied in terms of step. According to the load demand and the change of PV output, $P_{\text{FC}}, P_{\text{MS}}^{\text{ref}}, P_{\text{Feeder}}^{\text{ref}}$ and the operating mode were determined by the proposed operating algorithm. Fig. 8 shows the simulation results of the system operating strategy. The changes of P_{PV} and P_{Load} are shown in Fig. 8(a) (Δ line) and Fig. 8(b) (o, line), respectively.

Based on P_{PV} and the constraints of P_{FC} shown in Table I, the reference value of the hybrid source output $P_{\text{MS}}^{\text{ref}}$ is determined as dipicted in Fig. 8(a) (o line). From 0 s to 10 s, the PV operates at standard test conditions to generate constant power and, thus, $P_{\text{MS}}^{\text{ref}}$ is constant. From 10 s to 20 s, P_{PV} changes step by step and, thus, $P_{\text{MS}}^{\text{ref}}$ is defined as the algorithm shown in Fig. 4 or 5. The PEMFC ouput P_{FC}, as shown in Fig. 8(a) ($\bullet$ line), changes according to the change of P_{PV} and P_{MS}. Fig. 8(c) shows the system operating mode. The UPC mode and FFC mode correspond to values 0 and 1, respectively. From 4

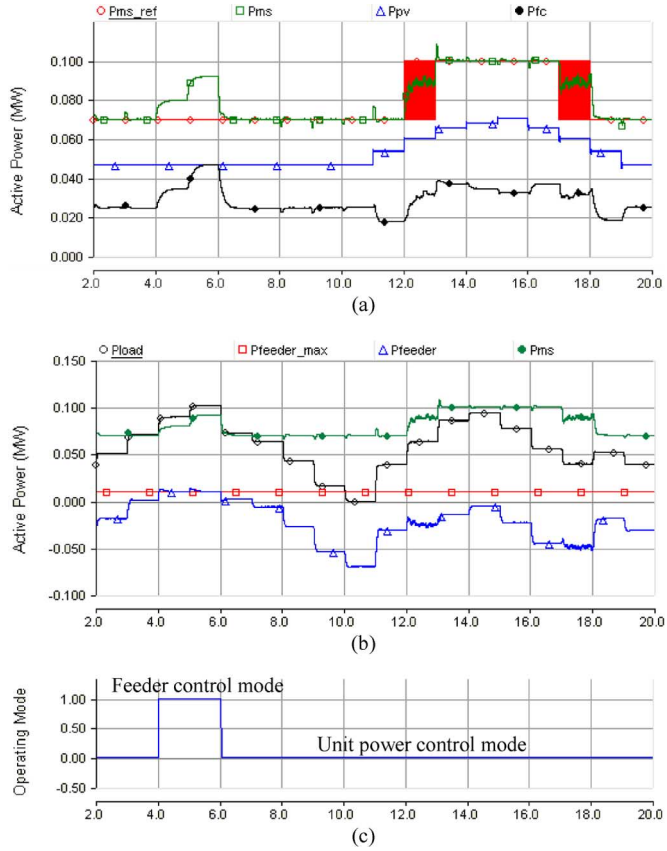

Fig. 8. Simulation result without hysteresis. (a) Operating strategy of the hybrid source. (b) Operating strategy of the whole system. (c) Change of operating modes.

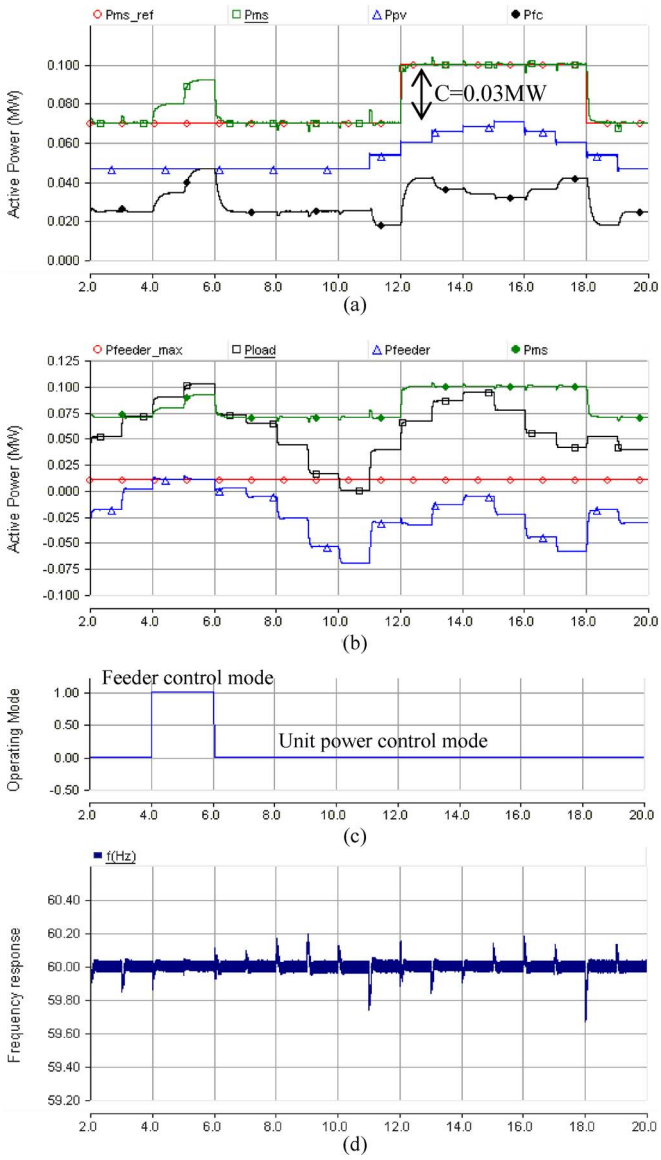

Fig. 9. Improving operation performance by using hysteresis: (a) The operating strategy of the hybrid source; (b) Operating strategy of the whole system. (c) Change of operating modes. (d) Frequency variations occur in the system.

s to 6 s, the system works in FFC mode and, thus, $P_{\text{Feeder}}^{\max}$ becomes the feeder reference value. During FFC mode, the hybrid source output power changes with respect to the change of load demand, as in Fig. 8(b). On the contrary, in UPC mode, P_{MS} changes following $P_{\text{MS}}^{\text{ref}}$, as shown in Fig. 8(a).

It can be seen from Fig. 8 that the system only works in FFC mode when the load is heavy. The UPC mode is the major operating mode of the system and, hence, the system works more stably.

It can also be seen from Fig. 8(a) that at 12 s and 17 s, $P_{\text{MS}}^{\text{ref}}$ changes continuously. This is caused by variations of P_{PV} in the MPPT process. As a result, P_{MS} and P_{FC} oscillate and are unstable. In order to overcome these drawbacks, a hysteresis was used to control the change of $P_{\text{MS}}^{\text{ref}}$, as shown in Fig. 6. The simulation results of the system, including the hysteresis, are depicted in Fig. 9.

B. Improving Operation Performance by Using Hysteresis

Fig. 9 shows the simulation results when hysteresis was included with the control scheme shown in Fig. 6. From 12 s to 13 s and from 17 s to 18 s, the variations of $P_{\text{MS}}^{\text{ref}}$ [Fig. 9(a), o line], FC output [Fig. 9(a), ● line], and feeder flow [Fig. 9(b), Δ line] are eliminated and, thus, the system works more stably compared to a case without hysteresis (Fig. 8). Fig. 9(d) shows the frequency variations when load changes or when the hybrid source reference power $P_{\text{MS}}^{\text{ref}}$ changes (at 12 s and 18 s). The parameter C was chosen at 0.03 MW and, thus, the frequency variations did not reach over its limit ($\pm 5\% * 60 = \pm 0.3$ Hz).

C. Discussion

It can be seen from Fig. 9(b) that during the UPC mode, the feeder flow (Δ line) changes due to the change of load (□ line) and hybrid source output (● line). This is because in the UPC mode, the feeder flow must change to match the load demand.

However, in a real-world situation, the microgrid should be a constant load from the utility viewpoint [17]. In reality, the microgrid includes some DGs connected in parallel to the feeder [13], [18]. Therefore, in the UPC mode, the changes of load will be compensated for by other FFC mode DGs and the power from the main grid will be controlled to remain constant.

In the case in which there is only one hybrid source connected to the feeder, the hybrid source must work in the FFC mode to maintain the feeder flow at constant. Based on the proposed

method, this can be accomplished by setting the maximum value of the feeder flow ($P_{\text{Feeder}}^{\max}$) to a very low value and, thus, the hybrid source is forced to work in the FFC mode. Accordingly, the FC output power must be high enough to meet the load demand when load is heavy and/or at night without solar power.

From the aforementioned discussions, it can be said that the proposed operating strategy is more applicable and meaningful to a real-world microgrid with multi DGs.

VI. Conclusion

This paper has presented an available method to operate a hybrid grid-connected system. The hybrid system, composed of a PV array and PEMFC, was considered. The operating strategy of the system is based on the UPC mode and FFC mode. The purposes of the proposed operating strategy presented in this paper are to determine the control mode, to minimize the number of mode changes, to operate PV at the maximum power point, and to operate the FC output in its high-efficiency performance band.

The main operating strategy, shown in Fig. 7, is to specify the control mode; the algorithm shown in Fig. 4 is to determine $P_{\text{MS}}^{\text{ref}}$ in the UPC mode. With the operating algorithm, PV always operates at maximum output power, PEMFC operates within the high-efficiency range ($P_{\text{FC}}^{\text{low}} \div P_{\text{FC}}^{\text{up}}$), and feeder power flow is always less than its maximum value ($P_{\text{Feeder}}^{\max}$). The change of the operating mode depends on the current load demand, the PV output, and the constraints of PEMFC and feeder power.

With the proposed operating algorithm, the system works flexibly, exploiting maximum solar energy; PEMFC works within a high-efficiency band and, hence, improves the performance of the system's operation. The system can maximize the generated power when load is heavy and minimizes the load shedding area. When load is light, the UPC mode is selected and, thus, the hybrid source works more stably.

The changes in operating mode only occur when the load demand is at the boundary of mode change (P_{Load1}); otherwise, the operating mode is either UPC mode or FFC mode. Besides, the variation of hybrid source reference power $P_{\text{MS}}^{\text{ref}}$ is eliminated by means of hysteresis. In addition, the number of mode changes is reduced. As a consequence, the system works more stably due to the minimization of mode changes and reference value variation.

In brief, the proposed operating algorithm is a simplified and flexible method to operate a hybrid source in a grid-connected microgrid. It can improve the performance of the system's operation; the system works more stably while maximizing the PV output power.

For further research, the operating algorithm, taking the operation of the battery into account to enhance operation performance of the system, will be considered. Moreover, the application of the operating algorithm to a microgrid with multiple feeders and DGs will also be studied in detail.

References

[1] T. Bocklisch, W. Schufft, and S. Bocklisch, "Predictive and optimizing energy management of photovoltaic fuel cell hybrid systems with short-time energy storage," in *Proc. 4th Eur. Conf. PV-Hybrid and Mini-Grid*, 2008, pp. 8–15.

[2] J. Larmine and A. Dicks, *Fuel Cell Systems Explained*. New York: Wiley, 2003.

[3] W. Xiao, W. Dunford, and A. Capel, "A novel modeling method for photovoltaic cells," in *Proc. IEEE 35th Annu. Power Electronics Specialists Conf.*, Jun. 2004, vol. 3, pp. 1950–1956.

[4] D. Sera, R. Teodorescu, and P. Rodriguez, "PV panel model based on datasheet values," in *Proc. IEEE Int. Symp. Industrial Electronics*, Jun. 4–7, 2007, pp. 2392–2396.

[5] C. Wang, M. H. Nehrir, and S. R. Shaw, "Dynamic models and model validation for PEM fuel cells using electrical circuits," *IEEE Trans. Energy Convers.*, vol. 20, no. 2, pp. 442–451, Jun. 2005.

[6] C. Hua and C. Shen, "Comparative study of peak power tracking techniques for solar storage system," in *Proc. 13th Annu. Applied Power Electronics Conf. Expo.*, Feb. 1998, vol. 2, pp. 679–685.

[7] A. Hajizadeh and M. A. Golkar, "Power flow control of grid-connected fuel cell distributed generation systems," *J. Elect. Eng. Technol.*, vol. 3, no. 2, pp. 143–151, 2008.

[8] C. Hua and J. R. Lin, "DSP-based controller application in battery storage of photovoltaic system," in *Proc.22nd IEEE Int. Conf. Industrial Electronics, Control, and Instrumentation*, Aug. 5–10, 1996, vol. 3, pp. 1750–1810.

[9] C. Hua, J. Lin, and C. Shen, "Implementation of a DSP-controlled photovoltaic system with peak power tracking," *IEEE Trans. Ind. Electron.*, vol. 45, no. 1, pp. 99–107, Feb. 1998.

[10] E. Koutroulism and K. Kaalitzakis, "Development of a microcontroller-based, photovoltaic maximum power point tracking control system," *IEEE Trans. Power Electron.*, vol. 16, no. 1, pp. 46–54, Jan. 2001.

[11] N. Mohan, T. M. Undeland, and W. P. Robbins, *Power Electronics, Converters, Applications and Design*, 2nd ed. New York: Wiley, 2003.

[12] R. H. Lasseter, "Microgrids," in *Proc. IEEE Power Eng. Soc. Winter Meeting*, Jan. 2002, vol. 1, pp. 305–308.

[13] R. H. Lasseter and P. Piagi, "Control and design of microgrid components," Jan. 2006, PSERC final project reports.

[14] P. Piagi and R. H. Lasseter, "Autonomous control of microgrids," presented at the Power IEEE Eng. Soc. General Meeting, Montreal, QC, Canada, 2006.

[15] F. Katiraei and M. R. Iravani, "Power management strategies for a microgrid with multiple distributed generation units," *IEEE Trans. Power Syst.*, vol. 21, no. 4, pp. 1821–1831, Nov. 2006.

[16] J. A. Peças Lopes, C. L. Moreira, and A. G. Madureira, "Defining control strategies for microgrids islanded operation," *IEEE Trans. Power Syst.*, vol. 21, no. 2, pp. 916–924, May 2006.

[17] H. Jiayi, J. Chuanwn, and X. Rong, "A review on distributed energy resources and microgrid," *Renew. Sustain. Energy Rev.*, vol. 12, pp. 2472–2483, 2008.

[18] M. Barnes, G. Ventakaramanan, J. Kondoh, R. Lasseter, H. Asano, N. Hatziargyriou, J. Oyarzabal, and T. Green, "Real-world microgrids—An overview," in *Proc. IEEE Int. Conf. System of Systems Engineering*, Apr. 16–18, 2007, pp. 1–8.

Loc Nguyen Khanh (S'09) was born in Vietnam on February 17, 1981. He received the B.S. and Master degrees in electrical engineering from Hanoi University of Technology, Hanoi, Vietnam, and is currently pursuing the Ph.D. degree at the School of Electrical Engineering at Inha University, Incheon, Korea.

His research interests include renewable energy, microgrid, and smartgrid.

Jae-Jin Seo was born in Korea on July 30, 1981. He received the B.S. degree in electrical engineering from Inha University, Incheon, Korea, and is currently pursuing the M.S. degree in electrical engineering at Inha University.

His research interests include fuel cells, distributed generation, and microgrid.

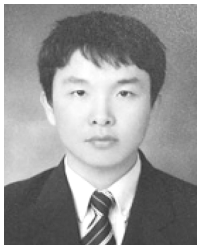

Yun-Seong Kim was born in Korea on May 26, 1982. He received the B.S. degree in electrical engineering from Inha University, Incheon, Korea.

Currently, he is a Master Course Student in the School of Electrical Engineering at Inha University. His research interests include power quality and distributed generation.

Dong-Jun Won (M'05) was born in Korea on January 1, 1975. He received the B.S., M.S., and Ph.D. degrees in electrical engineering from Seoul National University, Seoul, Korea, in 1998, 2000, and 2004, respectively.

He was a Postdoctoral Fellow with the APT Center, University of Washington, Seattle. Currently, he is an Assistant Professor with the School of Electrical Engineering, Inha University, Incheon, Korea. His research interests include power quality, microgrid, renewable energy, and hydrogen economy.